Journal of Materials Chemistry A

FEATURE ARTICLE

View Article Online
View Journal | View Issue

Cite this: J. Mater. Chem. A, 2014, 2, 1201

Recent advances of non-fullerene, small molecular acceptors for solution processed bulk heterojunction solar cells

Ala'a F. Eftaiha,[a] Jon-Paul Sun,[b] Ian G. Hill*[b] and Gregory C. Welch*[a]

Received 20th October 2013
Accepted 30th October 2013

DOI: 10.1039/c3ta14236a

www.rsc.org/MaterialsA

Organic, planar, and electron deficient small molecules were utilized as acceptors in the first reported bilayer heterojunction solar cells, however, current state-of-the-art organic photovoltaic (OPV) cells utilize fullerene derivatives as acceptor molecules. Recently, intensive efforts have been directed towards the development and understanding of soluble, non-fullerene, organic small molecules to fabricate bulk heterojunction (BHJ) solar cells. These efforts have been aimed at overcoming the inherent limitations of fullerene compounds such as the limited spectral breadth, air instability, and the typically higher production costs of fullerenes. In this focused review, we have highlighted the most recent progress over the last couple of years towards developing n-type organic small molecules utilized in BHJ devices in order to provide insight towards improving the overall performance of OPVs.

Introduction

Organic π-conjugated materials have the ability to conduct charge and absorb photons across the UV to near-IR regions of the solar spectrum. In addition, their large absorption coefficients, ease of engineering and processing, as well as low fabrication costs compared to inorganic semiconductors, make them potential candidates for developing photovoltaic (PV) cells.[1–5]

The conversion of solar energy into electricity in PV cells begins by photoexcitation of the semiconductor. This creates either free charges that move to their respective electrodes or electrically neutral, bound electron–hole states called excitons. If the intrinsic electric field within the cell is high enough, or the exciton binding energy is small compared to kT, the excitons can dissociate into free electrons and holes and migrate towards the cathode and the anode, respectively. Unfortunately, organic semiconductors typically have low relative dielectric constants ($\varepsilon \sim 3$), high exciton binding energies ($\gg$ kT at room temperature) as well as limited exciton diffusion lengths

[a]Department of Chemistry, Dalhousie University, 6274 Coburg Road, P.O. Box 15000, Halifax, Nova Scotia B3H 4R2, Canada. E-mail: gregory.welch@dal.ca; Tel: +1 902-494-4245

[b]Department of Physics, Dalhousie University, Halifax, Nova Scotia B3H 4R2, Canada. E-mail: ian.hill@dal.ca; Fax: +1 902-494-5191; Tel: +1 902-494-3897

Ala'a F. Eftaiha was born in Jerusalem, Palestine. He obtained his BSc and MSc in chemistry from the Hashemite University, Jordan. Ala'a carried out his graduate research under the supervision of both Dr Musa I. El-Barghouthi and Dr Adnan A. Badwan. After spending two years doing research at the Jordanian pharmaceutical Manufacturing Company, Jordan, he moved to Canada, where he completed his PhD in surface chemistry under the guidance of Dr Matthew F. Paige at the University of Saskatchewan. Recently, Ala'a has received an NSERC CREATE fellowship to carry out postdoctoral research at Dalhousie University, Canada.

Jon-Paul Sun is a PhD candidate in Physics at Dalhousie University. He obtained his BASc in Engineering Physics from the University of British Columbia where he researched laser locking techniques for atomic cooling applications in the Quantum Degenerate Gases Laboratory of Kirk W. Madison.

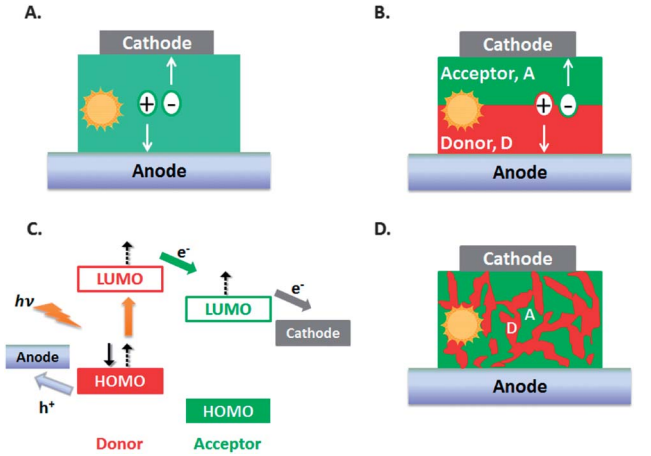

Fig. 1 Schematic illustration of (A) single layered organic solar cell, (B) planar-heterojunction device (PHJ), (C) exciton dissociation at the donor–acceptor heterojunction in organic solar cell and (D) bulk heterojunction solar cell. (B, C and D has been redrawn from Mishra and Bäuerle.[9])

(< 20 nm) that limit their usefulness for solar cell applications.[6] The power conversion efficiency (PCE) of single layered organic PVs (Fig. 1A) is typically less than 0.1%.[7,8]

The concept of heterojunction cells introduced by Tang[10] opened a new horizon in exploring organic semiconductors. The energetic offset between the HOMO–HOMO (highest occupied molecular orbital) and LUMO–LUMO (lowest unoccupied molecular orbital) at the donor–acceptor (D–A) interface, generated by stacking the materials between two electrodes in a planar-heterojunction device (PHJ, Fig. 1B), drives exciton dissociation, forming geminate pairs (Fig. 1C), with the electron in the acceptor, and the hole in the donor. Increased exciton dissociation and separation of holes and electrons reduced their recombination rate and thus improved the PCE of the PHJ. Nevertheless, the overall device efficiency is limited by the exciton diffusion length and small interfacial area at which the exciton dissociation takes place. These complications have been overcome by controlling the morphology of the D–A composite. It has been reported that an interpenetrating, bi-continuous network of phase separated D–A domains (BHJ, Fig. 1D) provides a high interfacial area for charge separation.[9,11–13] Controlling the size of D–A domains make it possible to enhance charge collection efficiency over recombination.[14–16]

The solution-processed active layer of BHJ devices ensures both low fabrication cost and simplicity (see the work by Li *et al.*[17] and others[18–21] for some examples). Such a process requires both the D–A molecules to be soluble in a common solvent. Herein, the processing solvent has a profound effect on the morphological characteristics and thereby, the optoelectronic properties of the active layer.[22–26]

It is of importance to make a connection between the physical parameters that affect the PCE in OPVs, including the open circuit voltage (V_{OC}) and the short circuit current (J_{SC}), with the molecular structure of the active layer. This can lead to better design strategies and enhance the competitiveness of OPVs with other thin-film technologies.

The PCE (η) is defined as the ratio of maximum device output power density (P_{out}) to the intensity of incident light (P_{in}) as follows

$$\eta = \frac{P_{out}}{P_{in}} = \frac{V_m J_m}{P_{in}} = \frac{V_{OC}\ J_{SC} FF}{P_{in}} \quad (1)$$

where V_m and J_m are the voltage and current at the maximum P_{out}, respectively, V_{OC} is open-circuit voltage; J_{SC} is short-circuit current density and FF is the fill factor.[9,27]

According to eqn (1), high PCE values are achieved by increasing the magnitude of V_{OC}, J_{SC} and FF. Although different strategies have been reported to control the device physics,[28–30] however, improvement of one or two of the parameters may require sacrificing the others. V_{OC} corresponds to the voltage at zero current density. It is limited by the energy difference between the HOMO and the LUMO levels of the D and A species, respectively. J_{SC} represents the maximum current that can be obtained

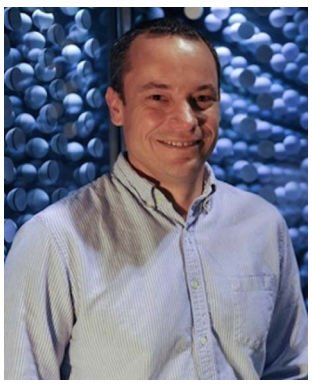

Ian Hill Professor at Dalhousie University in the Department of Physics and Atmospheric Science. Ian received his BSc in Engineering Physics and PhD in Physics from Queen's University (Kingston, Canada). Prior to joining the faculty at Dalhousie, Ian was a Visiting Research Fellow at Princeton University, a staff physicist at the US Naval Research Laboratory in Washington, DC, and a member of the technical staff at the Sarnoff Corporation (SRI International) in Princeton, NJ. His research interests include emerging photovoltaic technologies, organic and mixed metal oxide thin-film transistors, and interface engineering using self-assembled monolayers.

Gregory C. Welch is an Assistant Professor of Chemistry and Canada Research Chair at Dalhousie University in Halifax, Nova Scotia. He obtained a BSc in Chemistry from the University of Calgary in 2003 and worked in the laboratories of Tristram Chivers and Warren E. Piers. Gregory earned his PhD at University of Windsor in 2008 under the supervision of Douglas W. Stephan. He then moved to UC-Santa Barbara, where he worked as an NSERC postdoctoral fellow with Guillermo C. Bazan. His research interests focus in the area of Printed Electronics, where he is developing new functional materials.

when the voltage across the device is zero. FF is a parameter that describes how closely the cell behaves to a step-function ideal diode.[28,29] J_{SC} has been improved *via* exploiting low bandgap donor materials to harvest more sunlight, while V_{OC} has been increased by lowering the HOMO of the donor and reducing recombination between the donor and the acceptor.[31,32] It is often a challenge to improve both J_{SC} and V_{OC} simultaneously. For example, narrowing the donor bandgap (*i.e.*, achieving high J_{SC}) may be associated with a decrease in the V_{OC} of the device.

In order to improve the efficiency of solution processed BHJ OPVs, several different D–A classes have been explored. These include polymer/fullerene,[33] molecular donor (MD)/fullerenes[34–37] polymer/polymer,[38,39] polymer/molecular acceptor (MA)[40,41] and MD/MA.[42,43] In the following review, recent advances in different classes of D–A molecules for fabrication of BHJ solar cells that utilize non-fullerene small molecule acceptors (MA) is critically discussed. Moreover, the influence of the morphological aspect of the D–A composite on the device performance has been reviewed to illustrate the complex interplay between the active layer morphology and electronic properties, which are important in providing an in-depth understanding that will facilitate the design and development of high performance BHJ devices.

Polymer/fullerene BHJ OPV

Before we discuss the recent progress of non-fullerene small molecule based organic solar cells, it is important to recognize the importance of the polymer-fullerene solar cell, for which great successes have paved the way for new, and arguably improved, architectures. Conjugated, semiconducting polymers such as polythiophene, poly(*p*-paraphenylenevinylene) and their derivatives, particularly P3HT, MEH-PPV and MDMO-PPV (Fig. 2A and B) have attracted enormous attention for solar cell applications.[10,44–49] The photo-induced electronic characteristics of these polymers and both the high electron affinity, stability of Buckminsterfullerene[50] (or the most common soluble fullerene derivative PCBM,[51,52] Fig. 2C), and presence of low-lying anion excited states[53] provide a highly efficient, sub-picosecond, electron transfer process that represents a molecular approach to high efficiency photovoltaic conversion.[54–56] Furthermore, fullerenes have good electron mobilities[57,58] in three dimensions,[59] and can form favourable nanoscale phase separated domains in BHJs with a suitable selection of solvent additives.[60]

For efficient charge transfer, the minimum offset required between the LUMOs of the polymer and PCBM is about 0.3 eV. Therefore, the LUMO energy of an ideal donor should be approximately −3.9 eV (relative to −4.2 eV for the PCBM LUMO). To harvest solar photons effectively in the donor polymer, the HOMO energy should reside at approximately −5.4 eV to ensure strong absorption at 700 nm (the solar photon-flux maximum).[61,62]

Unfortunately, neither the substituted PPV ($E_g \sim 2.2$ eV) nor polythiophene ($E_g \sim 1.9$ eV) can effectively harvest photons from the solar spectrum. For example, P3HT is only capable of

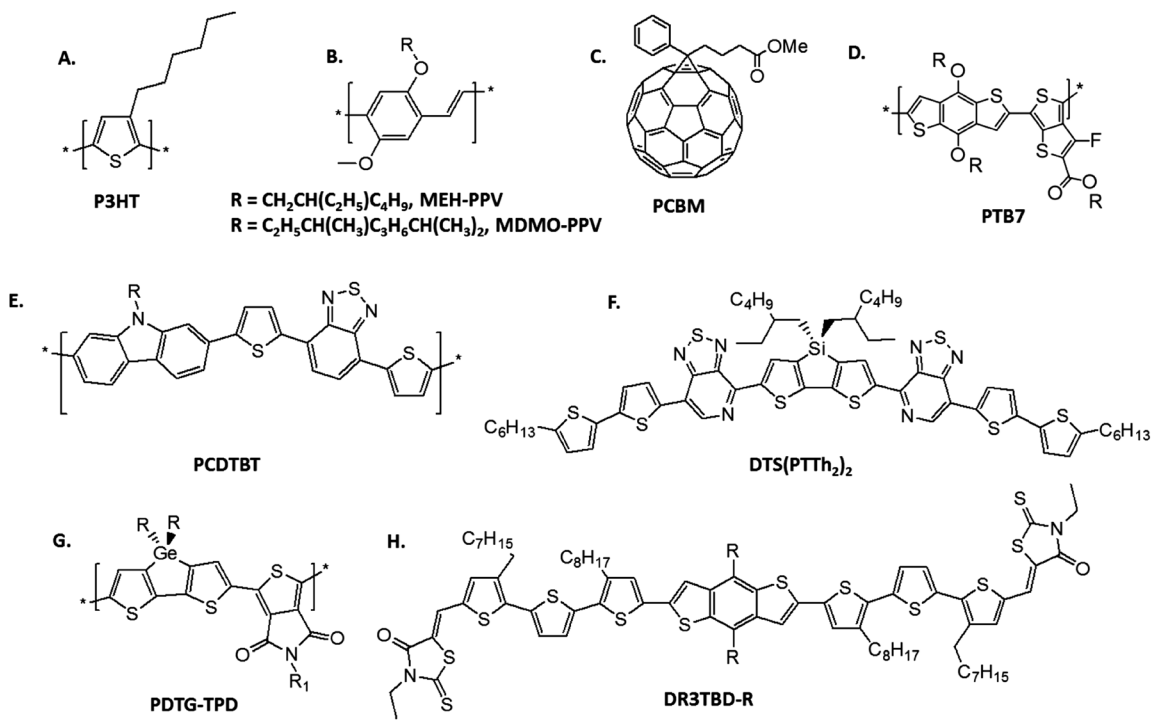

Fig. 2 Examples of organic semiconductors used as donors in OPVs, (A) poly(3-hexylthiophene), (B) poly[2-methoxy-5-(alkyl)-1,4-phenylen]-*alt*-(vinylene), (C) [6,6]-phenyl-C61-butyric acid methyl ester, (D) thieno[3,4-*b*]thiophene/benzodithiophene, (E) poly[*N*-9′′-hepta-decanyl-2,7-carbazole-*alt*-5,5-(4′,7′-di-2-thienyl-2′,1′,3′-benzothiadiazole)], (F) 5,5′-bisf(4-(7-hexylthiophen-2-yl)thiophen-2-yl) [1,2,5] thiadiazolo[3,4*c*] pyridineg-3,3′-di-2-ethylhexylsilylene-2,2′-bithiophene, (G) poly-dithienogermole-thienopyrrolodione and (H) benzo[1,2-*b*:4,5-*b*′]dithiophene (BDT) based donor molecules.

absorbing about 46% of the available solar photons. Lower-bandgap polymers (E_g < 1.8 eV) are required to increase the number of the absorbed photons.[63–65] Recently, low-bandgap polymers with light absorption extending to higher wavelengths have been developed (see Fig. 2D, E and G for examples). Over the past 3 years, the PCE of single layer devices incorporating these polymers have increased from 6 to 9% and over 10% for tandem cells.[20,31,61,66–74]

For polymer/fullerene composites, it has been found that BHJ solar cells offer one of the most successful device architectures developed to date.[13,18,20,75] (see the reviews by Thompson and Fréchet[27] and Li *et al.*[17] for more examples). Strategies other than the use of low-bandgap polymers can be exploited to improve the PCE. Optimizing the active layer morphology (including crystallinity and miscibility of D–A), exploiting higher fullerenes, and enhancing the solubility of fullerene derivatives are beyond the scope of this review. A number of these potential strategies have been discussed in the affiliated literature associated with polymer/fullerene OPV.[76,77]

Limitations to fullerene acceptors

Fullerenes have wide bandgaps and are weakly absorbing in the visible region of the solar spectrum, preventing complimentary light harvesting in acceptor domains. A good strategy for non-fullerene acceptors should address this deficiency by designing narrow bandgap materials with large extinction coefficients. While the P3HT:PCBM BHJ has served as a good platform for studying OPVs, moving to non-fullerene acceptors with tuneable energy levels will open up the field to a greater diversity of donor–acceptor pair combinations. Furthermore, in P3HT:PCBM BHJs, polar interactions cause PCBM to migrate towards the PEDOT:PSS interface.[78] Fullerene enrichment at the anode leads to decreased fracture resistance,[78] causing delamination of the active layer.[79] Clearly, the mechanical integrity of OPVs must be considered if they are to ever compete with their inorganic counterparts.

In terms of sustainability, a recent cradle-to-gate life cycle analysis by Landi *et al.*[80] reports the embodied energy of electronic grade PCBM to be 64.7 and 90.2 GJ kg^{-1} for C60 and C70, respectively, for synthesis *via* tetralin pyrolysis. Higher embodied energies were found for toluene feedstocks and plasma arc or plasma RF syntheses routes. The largest contributions to these exceptionally large embodied energies are the low yield and extensive organic solvent requirements. Typical OPV materials including P3HT have embodied energies one to two magnitudes lower.[81] New acceptor molecules need to be made from cheap building blocks with higher yield syntheses.

Small acceptor organic molecules

Organic molecules (donors and acceptors) have demonstrated the ability to replace both polymeric materials and fullerenes in fabrication of high efficiency BHJ OPVs.[82–84] This replacement has provided the opportunity to tailor low bandgap molecular structures with controlled absorption characteristics and HOMO–LUMO offsets to overcome some of the inherent drawbacks of polymer/fullerene BHJ devices, such as polymer molecular weight dependence and the poor photo-response of PCBM.[85–87]

Compared to polymer-based BHJ, small donor molecules (examples are shown in Fig. 2F and H (ref. 88 and 89)) offer well-defined molecular structures that reduce the batch-to-batch variability encountered with polymers. This makes the comparison between molecular-based BHJ fabricated in different laboratories, *via* different techniques, more reliable.[9,90,91] Additionally, high absorption coefficients, readily tuneable electronic energy levels, and easy synthesis make small acceptor molecules attractive replacements for fullerenes as electron acceptors.[92]

Very recently, MD architectures have emerged that combine facile and elegant synthesis, near ideal optical and electrochemical characteristics, and most importantly desirable film forming properties, leading to solar cell efficiencies of about 9% when employed as donors with fullerene acceptors (see the work by Gupta *et al.* and others[89,93,94] for some examples). These findings have provided important progress for the development of small organic molecules for use in solar cells. However, significant advances still need to be made, especially with respect to their use as fullerene replacements (acceptors) to develop air-stable and solution-processable n-type organic semiconducting materials. In the following section, we highlight recent advances of six classes of MAs constructed from combinations of simple weakly electron donating and strong electron accepting planar π-conjugated organic building blocks (donor–acceptor type materials) that provided molecular designs with high electron mobilities and tunable HOMO and LUMO energy levels that might be considered as a platform for fabricating high-performance organic solar cell devices. We recognize that several other classes of non-fullerene small molecules have been reported and utilized in OPV devices, including substituted pentacenes and 9,9-bifluroenylidenes,

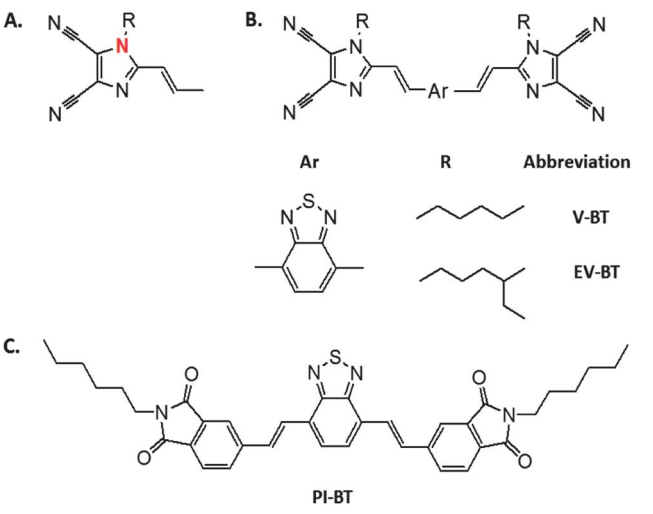

Fig. 3 Chemical structure of vinazene based acceptors (A) 1-alkyl-2-vinyl-4,5-dicyanoimidazole, (B) bis((1-alkyl-4,5-dicyanoimidazol-2-yl) vinyl) aryl compounds and (C) 4,7-bis(4-(*N*-hexyl-phthalimide)vinyl) benzo[*c*]1,2,5-thiadiazole (PI-BT).

and thus for a broader review of n-type organic materials, we refer the reader to reviews by Stolar and Baumgartner,[95] Gregoriou,[96] and Anthony.[97,98]

a. Vinazene based acceptors

Vinazene conjugated based materials synthesized from the Heck coupling reaction of 1-alkylvinazene (Fig. 3A) have been exploited as solution-processable n-type conjugated materials. These materials exhibit good film-forming properties, high optical densities, simple chemical synthesis and most importantly, the inherent structural flexibility offers tuning of their solubility and optoelectronic properties (absorption profile and HOMO–LUMO offset) either by changing the length of the alkyl group at N-1 position (Fig. 3A) or the central aromatic segments (Fig. 3B).[43,85,99–104]

In this context, planarity, conjugation length and electron-donating properties of the central aromatic group may cause either a blue or red shift in the absorption spectra of these compounds. For example, a phenylene bridged derivative has an absorption maximum at 376 nm. For more twisted derivatives, such as biphenylene or bi-naphthalene based compounds, the absorption maxima are blue-shifted to 369 and 362 nm respectively.

On the other hand, planar configurations such as a fluorene based central moiety, is red-shifted by 14 nm in comparison to the phenylene bridge derivative ($\lambda_{max} = 390$ nm). Incorporation of fused ring bridge moieties such as naphthalene, anthracene and tetracene, shifted λ_{max} to higher wavelengths relative to the phenylene bridge compounds. In a similar manner, red shifts in optical absorption have been observed for heterocyclic bridge building blocks such as bithienylene or thienothiophene.[101]

Among the several derivatives synthesized by Sellinger and co-workers, benzo[*c*]1,2,5-thiadiazole derivative (V-BT, Fig. 3B) represented a near ideal MA for use with polymeric donors such as P3HT and PPV derivatives. The absorption spectra of both V-BT (absorption maxima at 337 and 448 nm) and the polymers resulted in a photo-response spanning the range from 300 to 650 nm. Moreover, the high electron affinity of V-BT relative to the polymeric donors (the LUMO resides at approximately −3.49 eV) provided efficient charge transfer of the photo-generated electron from the donor polymer. It has been reported that optimizing the annealing conditions of the active layer made of either P3HT or PPV derivative and V-BT is important to control the cell performance, as D–A domain size was changed as function of annealing temperature. At 80 °C, the higher performance of the post-annealed active layer (PCE was increased from 0.07 to 0.45%) suggested the formation of a bi-continuous, percolating network that facilitates the transport of holes and electrons to the corresponding electrodes. This has been confirmed by atomic force microscopy (AFM) measurements that indicated the formation of phase-separated domains on the nanometer scale. Although the nanostructure of the post-annealed active layer contributed to a higher PCE compared to the as-cast film, the low J_{SC} and FF values (1.20 mA cm^{-2} and 0.35, respectively) imply non-optimal film morphology. At higher annealing temperatures (100 °C), the device efficiency dropped due to the formation of large domains (several hundred nanometres) that were larger than the exciton diffusion length.[85,99] The PCE was further increased to 1.1 and 1.4% upon using EV-BT (Fig. 3), the 2-ethylhexyl version of V-BT with P3HT and poly[3-(4-*n*-octyl)-phenylthiophene] (POPT) respectively in BHJ devices. It is worth mentioning that the solubility of branched alkylvinazene derivatives is superior to the hexyl version in more common organic solvents. Herein, the larger PCE values obtained for the POPT containing active layer has been attributed to the larger D–A separation distance afforded by the phenyl group of the polymer. This resulted in destabilization of the geminate pair, which led to more efficient charge separation in POPT/EV-BT devices.[102]

As mentioned before, the energy difference between the donor HOMO and the acceptor LUMO helps determine V_{OC} in high-efficiency solar cells. The relative high binding energy of the HOMO level of poly(2,7-carbazole) (−5.6 eV *versus* −3.6 eV of EV-BT LUMO) as well as its complementary absorption of the acceptor vinazene molecule suggested a higher attainable V_{OC} when compared to previously reported values of both P3HT or PPV derivatives and V-BT. BHJ devices made of poly(2,7-carbazole)/EV-BT blends exhibited a PCE of 0.75%, a V_{OC} greater than 1.3 V with low J_{SC} and FF (1.14 mA cm^{-2} and 0.49, respectively).[100] Moreover, the potential utility of vinazene based acceptors (both V-BT and EV-BT) in BHJ solar cells were tested with diketopyrrolopyrrole (DPP) based materials. Although the LUMO–LUMO offset between the donor DPP molecule and the vinazene acceptor provided enough driving force for charge separation and thus high V_{OC} and PCE (up to 1.25 V and 1.1%, respectively), AFM images indicated that blend morphology limits the device performance.[43]

The relatively low efficiencies of the devices incorporating the 2-ethyl hexyl vinazene based acceptors were attributed to the low electron mobility of EV-BT (two orders of magnitude smaller than PCBM). To increase the electron mobility, dicyanoimidazol

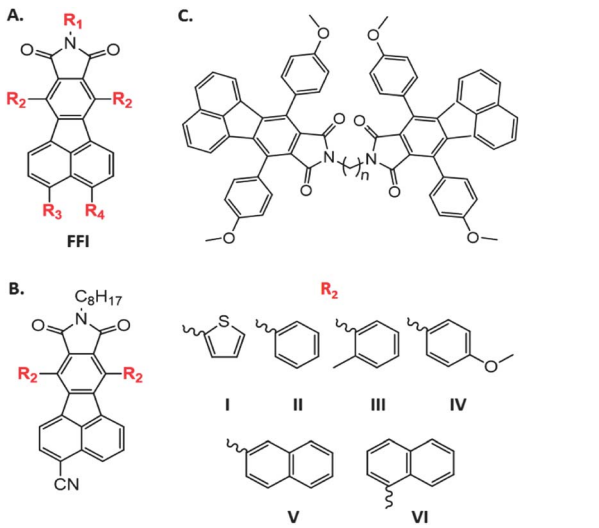

Fig. 4 Chemical structures of FFI based acceptors, (A) FFI building block, (B) different cyano- aryl-octyl derivatives of FFI and (C) example of FFI dimer.

groups have been replaced by electron deficient units such as vinyl imide. Bloking *et al.* reported a PCE of 2.54% for a solution-processed, P3HT/non-fullerene BHJ solar cell with a V_{OC} of 0.96 V for 4,7-bis(4-(*N*-hexyl-phthalimide)vinyl)benzo[*c*]1,2,5-thiadiazole (PI-BT, Fig. 3C) as MA.[105] The PI-BT acceptor was shown to contribute significantly to photo-current generation, and exhibited a strong tendency to form highly ordered domains appropriate for rapid electron transport.

b. Fluoranthene-fused imide (FFI) based acceptors

FFI derivatives (Fig. 4A) provided a platform to design air-stable and solution-processable MAs. This class of compounds is synthesized in several straight forward reaction steps using readily available starting materials. Condensation reactions between acenaphthequinone derivatives and 1,3 di-substituted acetone, followed by a Diels–Alder reaction between the produced cyclopentadienone and N-substituted pyrrole-2,5-dione with subsequent decarbonylation and oxidation give way to target materials. The photophysical and electrochemical properties of these compounds can be tuned by introducing electron withdrawing substituents that shift absorption maxima to lower wavelengths as well as reducing LUMO energies. These attributes enabled matching of the work function of different cathodes with the electron affinity of the different FFI derivatives and offered the potential to increase V_{OC} compared to fullerene based solar cell devices (their electron affinity is lower than that of PCBM).[106–108]

It has been reported that introducing electron withdrawing groups, particularly cyano groups, in a *para*-position relative to the largest π-conjugated core of the molecule, (R_3, Fig. 4A) is the most ideal scenario to lower the LUMO level of FFI acceptors.[106] In this context, Pei and co-workers reported a group of eight FFI based compounds whose LUMO levels ranged from −3.2 to −3.8 eV. The large variation in LUMO was based on both the strength, and the position, of the electron-withdrawing groups.

Initial results showed that the cyano-thiophenyl derivative (Fig. 4B.I) gave the best PCE of 1.86% in BHJs with P3HT as the electron donor. This decent PCE was achieved by controlling the speed of the solvent evaporation and applying a thermal annealing process to optimize grain size and phase separation within the active layer.[107] A further modification of the acceptor structure was performed by replacing the thiophenyl substituents with pendent aryl groups (Fig. 4B.II–IV). Although the LUMO levels of the aryl-based acceptors didn't change significantly (range from 3.40 to 3.48 eV), their blends with P3HT achieved PCEs higher than 2% in BHJ solar cells. The similar values of V_{OC} and FF of the five aryl based active layers (0.95 V and 0.50, respectively) implied that the differences in PCEs arise mainly from different J_{SC} values. Electron mobility data of the FFI-aryl derivatives indicated the highest electron mobility was recorded for the *ortho*-toluene derivative (Fig. 4B.III). This led to the highest J_{SC} and PCE (2.89%).[108]

The impact of alkyl-chain length (R_1 substituent, Fig. 4A) on the crystallinity of FFI dimers (Fig. 4C) have been explored by Ding *et al.* Results indicated that odd-carbon alkyl chains displayed a stronger one-dimensional growing tendency, different

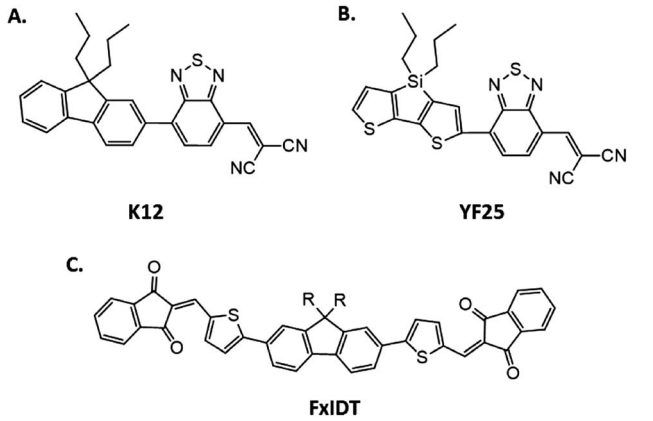

Fig. 5 Chemical structure of (A) 2-[(7-{9,9-di-n-propyl-9*H*-fluoren-2-yl}benzo[c][1,2,5]thiadiazol-4-yl)-methylene]malononitrile (K12) and (B) 2-[{7-(4,4-di-*n*-propyl-4*H*-silolo[3,2-*b*:4,5-*b*0]dithien-2-yl) benzo[c]-[1,2,5] thiadiazol-4-yl}methylene]malononitrile (YF25) and (C) FxIDT small molecule architecture. R = octyl (F8IDT) and R = 2-ethylhexyl (FEHIDT).

molecular configuration and increased crystallinity than those with even-carbon chains.[109] Further studies are still needed to examine the impact of both molecular configuration and crystallinity on the PCE of BHJ solar cells.

It has been reported the aryl substituents of cyano- aryl-octyl derivatives of FFI (R_2, Fig. 4B.I–VI) were almost perpendicular to the main plane of the molecule. This suggested a weak intermolecular π–π interaction that would suppress aggregation in the solid state. Although this led to amorphous structures accompanied by low electron mobility, devices containing FFI acceptors exhibited relatively high PCE values.[107,108]

c. Fluorene and dithienylsilole based acceptors

The Burn and Meredith research groups have reported an n-type organic semiconductor based on a FBT motif comprised of benzothiadiazole (BT), dicyanovinyl and 9,9-di-*n*-propylfluorene building blocks.[110] The backbone structure of the FBT motif provides both high electron affinity and processibility through the dicyanovinyl-benzothiadiazole and the di-*n*-propylated-fluorene units, respectively.[111] K12 shown in Fig. 5A is rapidly synthesized *via* a condensation reaction between brominated-BT and di-*n*-propylatedfluorene-boronic acid under Suzuki conditions, followed by Knoevenagel condensation of the produced aldehyde with malononitrile. The FBT-type molecule (K12) was found to have a similar electron affinity to PCBM and peak absorption as a thin-film at ~475 nm. The low lying LUMO and complimentary absorption profile compared to P3HT, made K12 a promising acceptor to be blended with P3HT.[110,112]

An optimized P3HT/K12 active layer achieved a PCE of 0.73% in BHJ device.[110] Annealing of the active layer improved the device performance by increasing both the surface roughness of the active layer and the electron mobility of K12. This has been confirmed independently by measuring the influence of annealing on as-cast K12 films.[112,113] Moreover, the contribution of K12 to the produced photo-current could be explained either

by energy transfer from the excited K12 to P3HT followed by electron transfer back to the acceptor (Channel I process) or by the photo-induced hole transfer (PHT) from K12 to P3HT (Channel II process).[110]

Coupling the dicyanovinyl-benzothiadiazole with di-*n*-propylated dithienylsilole unit has led to a narrow band gap MA (YF25, Fig. 5B) with a LUMO energy very close to that of PCBM (−3.7 eV) and a HOMO energy of −5.4 eV. The low band gap of YF25 enabled the D–A blends to absorb in the near infrared region of the solar spectrum. Replacing K12 with YF25 against P3HT doubled the PCE in a BHJ device.[114] The correlation between the thermal properties of binary mixtures comprised of P3HT and either K12 or YF25 and their optoelectronic performance in BHJ solar cells indicated that the maximum PCE and J_{SC} of both systems took place in the hypoeutectic mixture with respect to P3HT, as obtained from the differential scanning calorimetry measurements of the respective mixtures.[115]

Watkins and co-works just recently reported on a symmetrical derivative of K12 utilizing electron deficient indan-1,3-dione endcapping units in place of dicyanovinyl-benzothiadiazole.[116] The novel acceptors FxIDT (Fig. 5C), were readily synthesized *via* a set of Suzuki and Knoevenagel reactions in high yield from inexpensive starting materials. P3HT/FEHIDT (where EH = 2-ethylhexyl) based devices showed good PCE values up to 2.43% with large V_{OC} values approaching 1 V. These results are extremely promising due to the ease in which the acceptor molecules are synthesized from inexpensive materials. Importantly, the authors also demonstrated that analogues acceptors with linear octyl side chains (Fig. 5C, R = octyl) exhibit inferior performance as a result of stronger molecular coupling between molecules. This finding indicates the importance of side chain selection, in addition to energy level and bandgap alignment, when designing new materials to replace fullerene acceptors.

d. Oligothiophene-naphthalene diimide (NDI-nT(H)) acceptors and its analogs

The napthalene diimide conjugated aromatic heterocycle is a readily available and versatile building block that has been used to construct a range of high performance N-type materials.[117,118] The Jen research group has recently reported on the photophysical, electrochemical and charge transport properties of functionalized NDI-nT(H) oligomers (Fig. 6A) and evaluated their utility as acceptors in BHJ solar cells. These small molecules consist of a naphthalene dimiide (NDI) core flanked by thiophene end capping units. Such materials are synthesized by a reaction between 2,6-dibromonaphthalene diimide and alkyl substituted stannylthiophene using palladium catalysts. The NDI core ensures a low lying LUMO while the thiophene units extend π-conjugation leading to narrower optical band gaps. It is important to note that this architecture contains alkyl groups both perpendicular and parallel to the conjugated backbone allowing for fine control over both solubility and self-assembly properties.[119]

The size of the oligothiophene chains attached to the central naphthalene diimide building block played a major role in controlling the magnitude of both the absorption bands (525–683 nm) and the optical band gaps (varied from 2.1 to 1.4 eV). This demonstrated the potential utility of such regimes for light harvesting and exciton generation. The HOMO energy level of these oligomers could be tuned from −5.5 to −6.1 eV, keeping the LUMO energy level relatively constant (∼−4 eV). The maximum PCE using P3HT in BHJ devices was recorded for P3HT:NDI-3TH ($\eta = 1.5\%$) in the presence of 1,8-diiodooctane as a processing additive. The solvent additive was found to regulate both the domain size and connectivity of the NDI-3TH in the blends.[119,120] Although nanowire films of NDI-3TH showed a significant red-shift with enhanced intensity of the absorption band compared to NDI-3TH thin films, BHJ solar cells based on a nanowire blend of both P3HT and NDI-3TH showed a lower PCE of 1.15%.[121] Very recently, an analogous molecular structure to the electron deficient polycyclic rings of NDI-nT(H) that combine a superior intermolecular orbital overlap, improved carrier mobilities, optical and electronic properties as well as tunable electronic structure has been introduced by Jenekhe and co-workers. Tetraazabenzodifluoranthenediimides (Fig. 6B) combine large electron affinities (3.6–4.3 eV), optical band gaps of 2.5–1.6 eV and electron mobility of 0.12 $cm^2\ V^{-1}\ s^{-1}$ with a PCE of 1.8% in a BHJ device.[122]

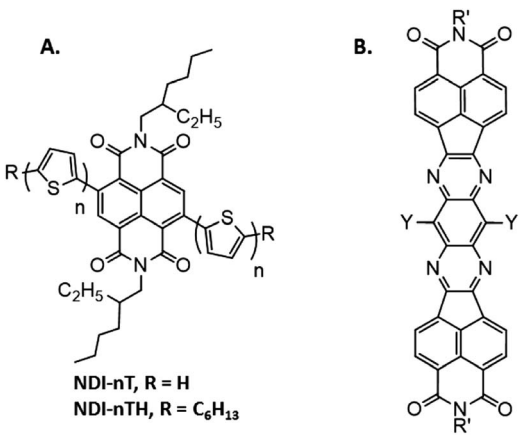

Fig. 6 The chemical structure of (A) oligothiophene-functionalized naphthalene diimide and (B) tetraazabenzodifluoranthenediimide.

e. Diketopyrrolopyrrole (DPP) based acceptors

Due to its strong light absorption, thermal stability and simple functionalization of the amide-nitrogen atom, the DPP chromophore (Fig. 7A) has had much success in electron donating materials for photovoltaic applications.[123–125] More recently, DPP-based acceptors paired with P3HT have been reported with PCEs reaching 2.05%.[53] The DPP core is commonly substituted at the 3 and 6 positions with thienyl (DPP(Th)$_2$) (Fig. 7B),[126] resulting in greater planarity of the molecular backbone and increased π–π interactions. These materials can be grouped into two molecular architectures; one with DPP as the central core, and the other with DPP as end-capping units (Fig. 7C–E).[53,124,127]

Chen and co-workers reported a series of four compounds with DPP(Th)$_2$ cores capped with fluorinated phenyl and phenyl-vinyl groups (Fig. 7C.I–IV).[126] The vinyl-containing

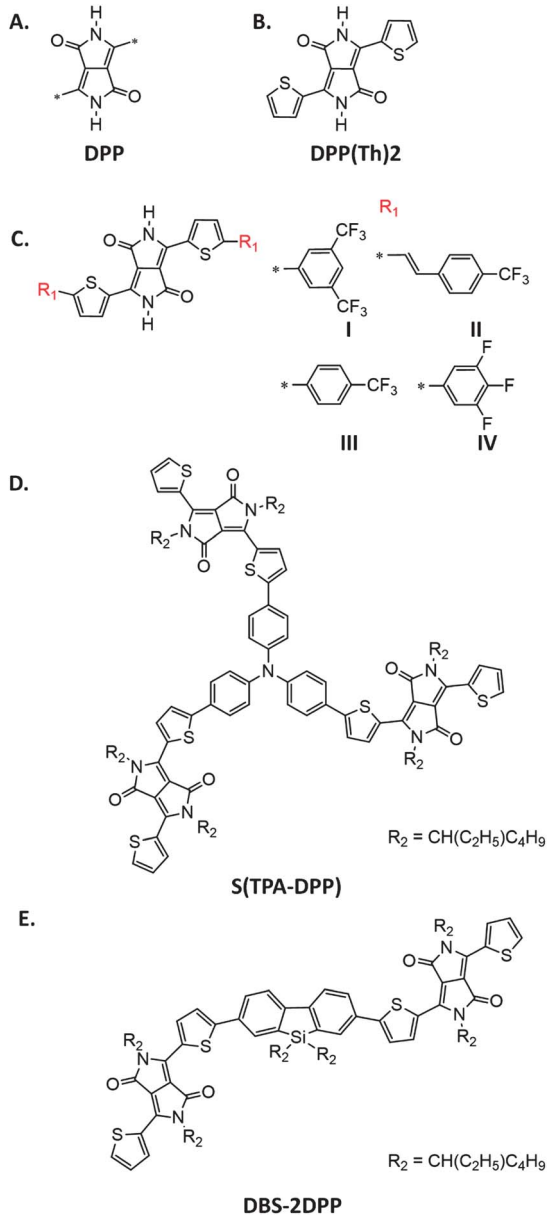

Fig. 7 The chemical structure of (A) DPP core, (B) DPP(Th)$_2$, (C) different π-DPP(TH)$_2$-π derivatives, (D) S(TPA-DPP), (E) DBS-2DPP. CH(C2H5)C4H9 = 2-ethylhexyl.

derivative showed a smaller optical bandgap (1.81 eV) due to the increased conjugation length and more planar structure. DFT calculations illustrated the vinyl-containing derivative containing a dihedral angle between the end-capping units of 5.33 degrees, in comparison to 17.96–22.46 degrees for the other three derivatives, all with similar optical bandgaps of 1.92–1.94 eV. The best performing molecule gave a PCE of 1.0% when blended with P3HT. Part of the relative success of this molecule is attributed to the higher LUMO level from comparatively weaker electron withdrawing substituents on the phenyl rings, leading to a larger V_{OC} of 0.81 V.

For DPP end-capped moieties, the Zhan group reported on a star-shaped triphenylamine core flanked by three DPP(Th)$_2$ units[127] (Fig. 7D). This compound displayed an optical bandgap of 1.85 eV and a high LUMO level (−3.26 eV). When combined with P3HT, a large V_{OC} of 1.18 V, J_{SC} 2.68 mA cm^{-2} and PCE 1.20% was achieved. Favourable nanoscale phase separation was confirmed by AFM, however low electron mobility (6.8×10^{-6} cm^2 V^{-1} s^{-1}) resulted in poor FF and J_{SC} (0.38 and 2.68 mA cm^{-2} respectively).

The same group recently reported on a dibenzosilole (DBS) core with two DPP(Th)$_2$ end-capping units[53] (Fig. 7E). The σ*-orbital of the silicon–carbon bond interacts with the π*-orbital of the butadiene, pulling down the LUMO level. The bulkiness of the silicon atom has little effect on the planarity of DBS, leading to promising electronic properties.[128,129] DBS-2DPP BHJ devices blended with P3HT resulted in V_{OC} of 0.97 V, J_{SC} 4.91 mA cm^{-2}, and PCE 2.05%. AFM images showed the films had interpenetrating networks with long fibrils 20 nm in diameter, indicating desirable phase separation. Based on these results, the DPP unit appears to be a promising building block for which to construct novel small molecule acceptors, due in part to the facile synthesis, long wavelength absorption, and low-lying LUMO levels. For further reading we direct the readers to a feature article by Qu and Tian[124] for a comprehensive review of DPP-based OPV materials.

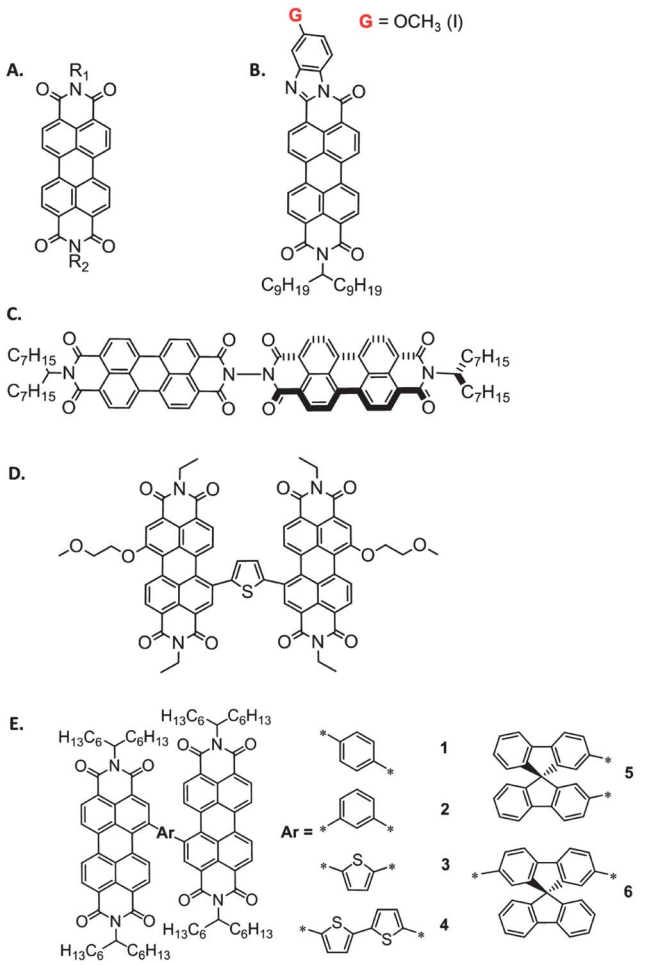

Fig. 8 The chemical structure of (A) perylenediimides, (B) perylene imide-imidazole, (C) non-planar perylenediimides molecules and (D) thienyllinked perylenediimide, (E) arylene linked PDI dimers.

f. Perylenediimide (PDI) acceptors

The optoelectronic characteristics, durability, ease of chemical functionalization and tendency for crystallization in solid films of PDI molecules (Fig. 8A), implied the potential utility of perylene core compounds as n-type semiconductors for BHJ solar cell applications.[130–132] Although the first bilayer solar cell reported in 1986 was comprised of a perylenetetracarboxylic derivative and a phthalocyanine,[10] the usefulness of PDI compounds in D–A blends were first reported in 1999.[133] In this context, substituted PDI molecules have been exploited to achieve solution processable derivatives as well as tailor the electronic and the optical properties of the functionalized perylene core compounds.[134]

One of the essential requirements for fabricating efficient PDI based devices is to exploit N-functionalized perylene compounds bearing small pendent groups such as N-dihexyl derivatives. This class of compounds exhibits good intermolecular packing, in contrast to those bearing bulky groups such as phenyl-di-*tert*-butyl.[135] This increases exciton diffusion lengths and thus achieves high charge separation efficiency, as well as reduces charge recombination at the D–A interface.[135–137] The thermal annealing of BHJ solar cells made of copper phthalocyanine and the N-dihexyl PDI derivative improved both the blend crystallinity and the charge carrier efficiency. This increased both the device PCE (from 0.15 to 0.52%) and J_{SC} values (the maximum value was 2.30 mA cm^{-2}).[138]

Compared to the symmetric PDI compounds, asymmetric perylene imide–imidazoles (Fig. 7B) exhibit a narrower energy bandgap. Interestingly, functionalizing the imidazole ring results in tuning solubility, frontier energy levels and light absorption patterns of these compounds.[139] The photoactive layer comprised of P3HT/benzimidazole-derived-imide–imidazole derivatives (Fig. 8B.I) achieved a PCE of 0.2% in a BHJ.[140]

One of the major explanations for the low efficiency of BHJ devices containing PDI molecules is the tendency of perylenes to undergo macro-crystallization from D–A blends. Therefore, reducing the perylene stacking without disturbing its charge-transport properties, may be used as a design principle. In this context, Narayan and co-workers showed that disruption of the perylene planarity by incorporating two perylene units perpendicular to each other's (Fig. 8C) could lead to PCEs of 2.77% when paired with a narrow band-gap benzo[1,2-*b*:4,5-*b*′]dithiophene based conjugated polymer. In comparison with planar PDI, a 10-fold increase in J_{SC} (9.5 mA cm^{-2}) was recorded.[131] In parallel with this discovery, very recently, Yao and co-workers have reported a thienyl linked PDI dimer (Fig. 8D), with reduced aggregation tendency, compared to the monomeric PDI (domain sizes ~30 nm compared to few hundred nanometers), that yielded the highest PCE value (4.03%) to date for a non-fullerene acceptor material when mixed with 5-alkylthiophene-2-yl-substituted BDT (Fig. 2H) bearing alkylcarbonyl-substituted thieno-[3,4-*b*]thiophene. The high J_{SC} value of the dimer PDI based devices (8.86 mA cm^{-2}) have been rationalized by the higher light-harvesting ability of the dimeric PDI compared to the monomeric PDI.[141]

Pei and co-workers have recently studied a series of PDI dimers having various arylene linkers to help uncover the relationship between molecular structure and electron mobility in non-fullerene based organic solar cells (Fig. 8E).[142] Their hypothesis was that bulk, sterically, encumbered dimeric PDI type structures would overcome the problematic self-aggregation and crystallization of planar, monomeric PDI base compounds. All compounds exhibited deep HOMO levels (*ca.* 5.7–5.8 eV), low lying LUMO levels (*ca.* 3.7–3.8 ev), and strong visible light absorption, appropriate for use as acceptors in OPV devices. The authors demonstrated that sterically hindered linkers such as 9,9′-spirobi[fluorene] (Fig. 8E, **5** and **6**) gave non-planar molecular structures with electron transport mobility values larger than planar thiophene, bithiophene and phenylene linkers. The higher mobilities were thought to arise from the formation of inter-connected, multi-dimensional, electron transporting networks. Solar cell efficiencies upwards of 2.3%, were reported for both compounds **5** and **6**, when coupled with P3HT.[142] Interestingly, all acceptors studied gave short-circuit currents >4 mA cm^{-2}, except compound **2**, with a *meta*-phenylene linker. X-ray diffraction, optical microscopy and fluorescence microscopy of P3HT:**2** thin films revealed a higher degree of crystallization and large scale phase separation, compared to thin films of P3HT with acceptors **1**, **3–6**. Modelling the structure of **2** using density functional theory revealed that the PDI units of **2** exhibit a nearly co-planar orientation, allowing **2** to undergo face-to-face stacking, a phenomenon not observed for the other structures. Thus the development of sterically hindered PDI derivatives that do not exhibit face-on stacking, is an effective strategy to overcome macro-crystallization of the D–A blends, allow for appropriate BHJ morphologies, and yield respectable PCEs.

Although the performance of MDs and MAs in BHJ derives are tested using fullerene derivatives and polymers respectively, Bazan and co-workers demonstrated that paring p-DTS(FBTTh$_2$)$_2$ and N-di(pentan-3-yl)-PDI derivative (Fig. 2F and 8A respectively) instead of phenyl-C$_{71}$-butyric acid methyl ester produced one of the highly efficient BHJ solar cells with a PCE of 3.0%.[42] The lower PCE of 3% compared to 7% for the fullerene based device was attributed to a lower J_{SC} and FF. Light intensity dependant revealed geminate recombination to be the primary loss mechanism. None-the-less, this work demonstrates the potential of small molecule:non-fullerene solution processed OPVs.

A recent review article by Kozma and Catellani provides a more comprehensive and historical overview of PDI-based OPVs.[130]

Conclusions

Small organic molecules are a viable alternative to polymers/fullerene compositions in BHJ solar cells. However, much less attention has been given to the operational performance and stability of organic molecular acceptor materials compared to their donor counterparts.[98]

In this review, we have highlighted the recent advances in exploiting several classes of molecular acceptors in BHJ solar cells. This summary might be used as a baseline for the researcher in this field to develop soluble molecular acceptors that combine a facile and elegant synthesis, near ideal optical

and electrochemical characteristics, and most importantly desirable film forming properties for use in solar cells as fullerene replacements.

Recent literature reports have indicated that great progress has been made in design and synthesis of small molecules with appropriate HOMO–LUMO energy levels and absorption profiles for use as acceptors in BHJ solar cells. The limiting factor in achieving high PCE values comparable to fullerene based systems, primarily lies within the active layer morphology, where it has been difficult to form well-ordered interpenetrating networks of donor and acceptor. These issues primary arise from either the donor or acceptor being too miscible in one another or over crystallization of one or both components. To overcome this obstacle, very recent result have shown that decreasing the molecular planarity, and thus tendency to crystallize, has led to impressive efficiency of 4%, more effort in this area is required. In this regard, the tendency of the molecular acceptor to form smaller aggregates increases the D–A interfacial area and thus contributes to the high device performance. This recurring theme of the ability to form phase separated domains on the order of exciton diffusion length has been demonstrated throughout successful non-fullerene acceptors in the literature.

Therefore, in-addition to the guidelines outlined by Anthony *et al.*[98] to design stable acceptor molecules with high electron mobilities, one major direction that might be gleaned from recent literature is to explore non-planar molecules[131,141] (such as those shown in Fig. 7C and D) that showed superior device performance over planar structures. Moreover, it is suggested to functionalize the acceptor molecules with fluoroalkyl side chains to tune the morphology of BHJ blends. In this context, fluorinated chains enable both lateral and vertical phase separation when blended with fully hydrogenated donor molecules, which lead to high performance devices.[143,144]

With the recent increases in PCE from 2 to 4% for OPVs based upon non-fullerene small molecules over the past few years, and the growing number of researchers in this field, it is fully expected that PCEs will continue to rise and possibly match that of fullerene based cells in the not too distant future. Indeed OPVs using polymer based acceptors have recently been reported to have PCEs in excess of 6%.[38] While it is beyond the scope of this review, we strongly encourage researchers to consider reporting a cost-analysis[145] of newly synthesized small molecule acceptors, as quoting the high cost of fullerenes is a recurring theme and motivational driving force for this field.

As a final comment, it is intriguing that the first reported heterojunction solar cell was comprised of a molecular donor and non-fullerene acceptor, and that today, twenty seven years later, this same architecture (albeit now solution processed) is once again receiving significant attention from the solar cell community.

Acknowledgements

A.F.E is grateful for the receipt of an NSERC CREATE DREAMS fellowship (Dalhousie Research in Energy, Advanced Materials and Sustainability, http://dreams.irm.dal.ca/). I.H and G.C.W acknowledge the NSERC Discovery Program for financial support. Arthur Hendsbee is acknowledged for assisting with the editing of this manuscript.

References

1 S. Guenes, H. Neugebauer and N. S. Sariciftci, *Chem. Rev.*, 2007, **107**, 1324–1338, DOI: 10.1021/cr050149z.
2 Y. Cheng, S. Yang and C. Hsu, *Chem. Rev.*, 2009, **109**, 5868–5923, DOI: 10.1021/cr900182s.
3 B. Kippelen and J. Bredas, *Energy Environ. Sci.*, 2009, **2**, 251–261, DOI: 10.1039/b812502n.
4 F. G. Brunetti, R. Kumar and F. Wudl, *J. Mater. Chem.*, 2010, **20**, 2934–2948, DOI: 10.1039/b921677d.
5 A. Facchetti, *Chem. Mater.*, 2011, **23**, 733–758, DOI: 10.1021/cm102419z.
6 P. Würfel, *Physics of Solar Cells: From Basic Principles to Advanced Concepts*, Willey-VCH Verlag GmbH & Co., KGaA, Weinheim, 2nd edn, 2009.
7 H. Spanggaard and F. Krebs, *Sol. Energy Mater. Sol. Cells*, 2004, **83**, 125–146, DOI: 10.1016/j.solmat.2004.02.021.
8 H. Hoppe and N. S. Sariciftci, *J. Mater. Res.*, 2004, **19**, 1924–1945, DOI: 10.1557/jmr.2004.0252.
9 A. Mishra and P. Bäuerle, *Angew. Chem., Int. Ed.*, 2012, **51**, 2020–2067, DOI: 10.1002/anie.201102326.
10 C. W. Tang, *Appl. Phys. Lett.*, 1986, **48**, 183–185, DOI: 10.1063/1.96937.
11 J. J. M. Halls, C. A. Walsh, N. C. Greenham, E. A. Marseglia, R. H. Friend, S. C. Moratti and A. B. Holmes, *Nature*, 1995, **376**, 498–500, DOI: 10.1038/376498a0.
12 G. Yu and A. J. Heeger, *J. Appl. Phys.*, 1995, **78**, 4510–4515, DOI: 10.1063/1.359792.
13 G. Yu, J. Gao, J. C. Hummelem, F. Wudl and A. J. Heeger, *Science*, 1995, **270**, 1789–1791, DOI: 10.1126/science.270.5243.1789.
14 B. A. Collins, Z. Li, J. R. Tumbleston, E. Gann, C. R. McNeill and H. Ade, *Adv. Energy Mater.*, 2013, **3**, 65–74, DOI: 10.1002/aenm.201200377.
15 M. T. Dang, L. Hirsch, G. Wantz and J. D. Wuest, *Chem. Rev.*, 2013, **113**, 3734–3765, DOI: 10.1021/cr300005u.
16 C. J. Takacs, Y. Sun, G. C. Welch, L. A. Perez, X. Liu, W. Wen, G. C. Bazan and A. J. Heeger, *J. Am. Chem. Soc.*, 2012, **134**, 16597–16606, DOI: 10.1021/ja3050713.
17 G. Li, V. Shrotriya, J. Huang, Y. Yao, T. Moriarty, K. Emery and Y. Yang, *Nat. Mater.*, 2005, **4**, 864–868, DOI: 10.1038/nmat1500.
18 S. Shaheen, C. J. Brabec, N. S. Sariciftci, F. Padinger, T. Fromherz and J. C. Hummelen, *Appl. Phys. Lett.*, 2001, **78**, 841–843, DOI: 10.1063/1.1345834.
19 W. L. Ma, C. Y. Yang, X. Gong, K. Lee and A. J. Heeger, *Adv. Funct. Mater.*, 2005, **15**, 1617–1622, DOI: 10.1002/adfm.200500211.
20 J. M. Kroon, M. M. Wienk, W. J. H. Verhees and J. Hummelen, *Thin Solid Films*, 2002, **403**, 223–228, DOI: 10.1016/S0040-6090(01)01589-9.
21 M. Kaltenbrunner, M. S. White, E. D. Glowacki, T. Sekitani, T. Someya, N. S. Sariciftci and S. Bauer, *Nat. Commun.*, 2012, **3**, 770, DOI: 10.1038/ncomms1772.

22 D. T. Duong, B. Walker, J. Lin, C. Kim, J. Love, B. Purushothaman, J. E. Anthony and T. Nguyen, *J. Polym. Sci., Part B: Polym. Phys.*, 2012, **50**, 1405–1413, DOI: 10.1002/polb.23153.

23 L. Ye, S. Zhang, W. Ma, B. Fan, X. Guo, Y. Huang, H. Ade and J. Hou, *Adv. Mater.*, 2012, **24**, 6335–6341, DOI: 10.1002/adma.201202855.

24 J. Peet, J. Y. Kim, N. E. Coates, W. L. Ma, D. Moses, A. J. Heeger and G. C. Bazan, *Nat. Mater.*, 2007, **6**, 497–500, DOI: 10.1038/nmat1928.

25 M. Campoy-Quiles, T. Ferenczi, T. Agostinelli, P. G. Etchegoin, Y. Kim, T. D. Anthopoulos, P. N. Stavrinou, D. D. C. Bradley and J. Nelson, *Nat. Mater.*, 2008, **7**, 158–164, DOI: 10.1038/nmat2102.

26 A. Pivrikas, H. Neugebauer and N. S. Sariciftci, *Sol. Energy*, 2011, **85**, 1226–1237, DOI: 10.1016/j.solener.2010.10.012.

27 B. C. Thompson and J. M. J. Fréchet, *Angew. Chem., Int. Ed.*, 2008, **47**, 58–77, DOI: 10.1002/anie.200702506.

28 W. J. Potscavage Jr, A. Sharma and B. Kippelen, *Acc. Chem. Res.*, 2009, **42**, 1758–1767, DOI: 10.1021/ar900139v.

29 Z. He, C. Zhong, X. Huang, W. Wong, H. Wu, L. Chen, S. Su and Y. Cao, *Adv. Mater.*, 2011, **23**, 4636–4643, DOI: 10.1002/adma.201103006.

30 K. Maturová, S. S. S. van Bavel, M. M. Wienk, R. A. J. Janssen and M. Kemerink, *Adv. Funct. Mater.*, 2011, **21**, 261–269, DOI: 10.1002/adfm.201001515.

31 H. Chen, J. Hou, S. Zhang, Y. Liang, G. Yang, Y. Yang, L. Yu, Y. Wu and G. Li, *Nature Photonics*, 2009, **3**, 649–653, DOI: 10.1038/nphoton.2009.192.

32 K. Vandewal, K. Tvingstedt, A. Gadisa, O. Inganas and J. V. Manca, *Nat. Mater.*, 2009, **8**, 904–909, DOI: 10.1038/nmat2548.

33 G. Li, R. Zhu and Y. Yang, *Nature Photonics*, 2012, **6**, 153–161, DOI: 10.1038/nphoton.2012.11.

34 B. Walker, A. Tamayo, D. T. Duong, X. Dang, C. Kim, J. Granstrom and T. Nguyen, *Adv. Energy Mater.*, 2011, **1**, 221–229, DOI: 10.1002/aenm.201000054.

35 Q. Huang and H. Li, *Chin. Sci. Bull.*, 2013, **58**, 2677–2685, DOI: 10.1007/s11434-013-5930-z.

36 J. E. Coughlin, Z. B. Henson, G. C. Welch and G. C. Bazan, *Acc. Chem. Res.*, 2013, DOI: 10.1021/ar400136b.

37 Y. Chen, X. Wan and G. Long, *Acc. Chem. Res.*, 2013, DOI: 10.1021/ar400088c.

38 A. Facchetti, *Mater. Today*, 2013, **16**, 123–132, DOI: 10.1016/j.mattod.2013.04.005.

39 C. R. McNeill, *Energy Environ. Sci.*, 2012, **5**, 5653–5667, DOI: 10.1039/c2ee03071c.

40 J. E. Anthony, *Chem. Mater.*, 2011, **23**, 583–590, DOI: 10.1021/cm1023019.

41 P. Hudhomme, *EPJ Photovoltaics*, 2013, **4**, 40401, DOI: 10.1051/epjpv/2013020.

42 A. Sharenko, C. M. Proctor, T. S. van der Poll, Z. B. Henson, T. Nguyen and G. C. Bazan, *Adv. Mater.*, 2013, **25**, 4403–4406, DOI: 10.1002/adma.201301167.

43 B. Walker, X. Han, C. Kim, A. Sellinger and T.-Q. Nguyen, *ACS Appl. Mater. Interfaces*, 2012, **4**, 244–250, DOI: 10.1021/am201304e.

44 A. Tsumura, H. Koezuka and T. Ando, *Appl. Phys. Lett.*, 1986, **49**, 1210–1212, DOI: 10.1063/1.97417.

45 F. Ebisawa, T. Kurokawa and S. Nara, *J. Appl. Phys.*, 1983, **54**, 3255–3259, DOI: 10.1063/1.332488.

46 I. Murase, T. Ohnishi, T. Noguchi, M. Hirooka and S. Murakami, *Mol. Cryst. Liq. Cryst.*, 1985, **118**, 333–336, DOI: 10.1080/00268948508076235.

47 F. Wudl and G. Srdanov, Conducting polymer formed of poly(2-methoxy-5-(2′-ethylhexyloxy)-*p*-phenylene vinylene), US pat., 5,189,136, 1993.

48 F. Padinger, R. Rittberger and N. Sariciftci, *Adv. Funct. Mater.*, 2003, **13**, 85–88, DOI: 10.1002/adfm.200390011.

49 A. N. Aleshin, *Phys. Solid State*, 2007, **49**, 2015–2033, DOI: 10.1134/s1063783407110017.

50 P. Allemand, A. Koch, F. Wudl, Y. Rubin, F. Diederich, M. Alvarez, S. Anz and R. Whetten, *J. Am. Chem. Soc.*, 1991, **113**, 1050–1051, DOI: 10.1021/ja00003a053.

51 F. Wudl, *Acc. Chem. Res.*, 1992, **25**, 157–161, DOI: 10.1021/ar00015a009.

52 S. Güenes, H. Neugebauer and N. S. Sariciftci, *Chem. Rev.*, 2007, **107**, 1324–1338, DOI: 10.1021/cr050149z.

53 Y. Lin, Y. Li and X. Zhan, *Adv. Energy Mater.*, 2013, **3**, 724–728, DOI: 10.1002/aenm.201200911.

54 N. S. Sariciftci, L. Smilowitz, A. J. Heeger and F. Wudl, *Science*, 1992, **258**, 1474–1476, DOI: 10.1126/science.258.5087.1474.

55 C. Lee, G. Yu, D. Moses, K. Pakbaz, C. Zhang, N. S. Sariciftci, A. J. Heeger and F. Wudl, *Phys. Rev. B: Condens. Matter Mater. Phys.*, 1993, **48**, 15425–15433, DOI: 10.1103/physrevb.48.15425.

56 G. Yu, K. Pakbaz and A. Heeger, *Appl. Phys. Lett.*, 1994, **64**, 3422–3424, DOI: 10.1063/1.111260.

57 E. von Hauff, V. Dyakonov and R. Parisi, *Sol. Energy Mater. Sol. Cells*, 2005, **87**, 149–156, DOI: 10.1016/j.solmat.2004.06.014.

58 P. H. Woebkenberg, D. D. C. Bradley, D. Kronholm, J. C. Hummelen, D. M. de Leeuw, M. Coelle and T. D. Anthopoulos, *Synth. Met.*, 2008, **158**, 468–472, DOI: 10.1016/j.synthmet.2008.03.016.

59 D. Guldi, *Chem. Commun.*, 2000, 321–327, DOI: 10.1039/a907807j.

60 H. Xin, X. Guo, G. Ren, M. D. Watson and S. A. Jenekhe, *Adv. Energy Mater.*, 2012, **2**, 575–582, DOI: 10.1002/aenm.201100718.

61 C. Soci, I. Hwang, D. Moses, Z. Zhu, D. Waller, R. Gaudiana, C. J. Brabec and A. J. Heeger, *Adv. Funct. Mater.*, 2007, **17**, 632–636, DOI: 10.1002/adfm.200600199.

62 L. J. A. Koster, V. D. Mihailetchi and P. W. M. Blom, *Appl. Phys. Lett.*, 2006, **88**, 093511, DOI: 10.1063/1.2181635.

63 C. J. Brabec, C. Winder, N. S. Sariciftci, J. C. Hummelen, A. Dhanabalan, P. A. van Hal and R. A. J. Janssen, *Adv. Funct. Mater.*, 2002, **12**, 709–712, DOI: 10.1002/1616-3028(20021016)12:10<709:aid-adfm709>3.0.co;2-n.

64 C. Winder, G. Matt, J. Hummelen, R. Janssen, N. Sariciftci and C. Brabec, *Thin Solid Films*, 2002, **403**, 373–379, DOI: 10.1016/s0040-6090(01)01588-7.

65 N. Z. Yahya and M. Rusop, *J. Nanomater.*, 2012, DOI: 10.1155/2012/793679.
66 N. Blouin, A. Michaud and M. Leclerc, *Adv. Mater.*, 2007, **19**, 2295–2300, DOI: 10.1002/adma.200602496.
67 S. H. Park, A. Roy, S. Beaupre, S. Cho, N. Coates, J. S. Moon, D. Moses, M. Leclerc, K. Lee and A. J. Heeger, *Nature Photonics*, 2009, **3**, 297–302.
68 Z. He, C. Zhong, S. Su, M. Xu, H. Wu and Y. Cao, *Nature Photonics*, 2012, **6**, 591–595, DOI: 10.1038/nphoton.2012.190.
69 C. E. Small, S. Chen, J. Subbiah, C. M. Amb, S. Tsang, T. Lai, J. R. Reynolds and F. So, *Nature Photonics*, 2012, **6**, 115–120.
70 L. Dou, J. You, J. Yang, C. Chen, Y. He, S. Murase, T. Moriarty, K. Emery, G. Li and Y. Yang, *Nature Photonics*, 2012, **6**, 180–185, DOI: 10.1038/nphoton.2011.356.
71 G. Li, R. Zhu and Y. Yang, *Nature Photonics*, 2012, **6**, 153–161, DOI: 10.1038/nphoton.2012.11.
72 J. You, L. Dou, K. Yoshimura, T. Kato, K. Ohya, T. Moriarty, K. Emery, C. Chen, J. Gao, G. Li and Y. Yang, *Nat. Commun.*, 2013, **4**, 1446, DOI: 10.1038/ncomms2411.
73 J. You, C. Chen, Z. Hong, K. Yoshimura, K. Ohya, R. Xu, S. Ye, J. Gao, G. Li and Y. Yang, *Adv. Mater.*, 2013, **25**, 3973–3978, DOI: 10.1002/adma.201300964.
74 X. Guo, N. Zhou, S. J. Lou, J. Smith, D. B. Tice, J. W. Hennek, R. P. Ortiz, J. T. L. Navarrete, S. Li, J. Strzalka, L. X. Chen, R. P. H. Chang, A. Facchetti and T. J. Marks, *Nature Photonics*, 2013, **7**, 825–833, DOI: 10.1038/nphoton.2013.207.
75 M. Svensson, F. Zhang, S. Veenstra, W. Verhees, J. Hummelen, J. Kroon, O. Inganas and M. Andersson, *Adv. Mater.*, 2003, **15**, 988–991, DOI: 10.1002/adma.200304150.
76 J. A. Bartelt, Z. M. Beiley, E. T. Hoke, W. R. Mateker, J. D. Douglas, B. A. Collins, J. R. Tumbleston, K. R. Graham, A. Amassian, H. Ade, J. M. J. Fréchet, M. F. Toney and M. D. McGehee, *Adv. Energy Mater.*, 2013, **3**, 364–374, DOI: 10.1002/aenm.201200637.
77 K. Kim, H. Kang, H. J. Kim, P. S. Kim, S. C. Yoon and B. J. Kim, *Chem. Mater.*, 2012, **24**, 2373–2381, DOI: 10.1021/cm3010369.
78 V. Brand, C. Bruner and R. H. Dauskardt, *Sol. Energy Mater. Sol. Cells*, 2012, **99**, 182–189, DOI: 10.1016/j.solmat.2011.11.035.
79 S. R. Dupont, M. Oliver, F. C. Krebs and R. H. Dauskardt, *Sol. Energy Mater. Sol. Cells*, 2012, **97**, 171–175, DOI: 10.1016/j.solmat.2011.10.012.
80 A. Anctil, C. W. Babbitt, R. P. Raffaelle and B. J. Landi, *Environ. Sci. Technol.*, 2011, **45**, 2353–2359, DOI: 10.1021/es103860a.
81 A. Anctil, C. W. Babbitt, R. P. Raffaelle and B. J. Landi, *Prog. Photovoltaics: Res. Appl.*, 2013, **21**, 1541–1554, DOI: 10.1002/pip.2226.
82 J. Roncali, *Acc. Chem. Res.*, 2009, **42**, 1719–1730, DOI: 10.1021/ar900041b.
83 N. Espinosa, R. Garcia-Valverde and F. C. Krebs, *Energy Environ. Sci.*, 2011, **4**, 1547–1557, DOI: 10.1039/c1ee01127h".
84 T. Liu and A. Troisi, *Adv. Mater.*, 2013, **25**, 1038–1041, DOI: 10.1002/adma.201203486.
85 T. Kietzke, R. Y. C. Shin, D. A. M. Egbe, Z. Chen and A. Sellinger, *Macromolecules*, 2007, **40**, 4424–4428, DOI: 10.1021/ma0706273.
86 K. H. Hendriks, G. H. L. Heintges, V. S. Gevaerts, M. M. Wienk and R. A. J. Janssen, *Angew. Chem., Int. Ed.*, 2013, **52**, 8341–8344, DOI: 10.1002/anie.201302319.
87 Z. B. Henson, K. Muellen and G. C. Bazan, *Nat. Chem.*, 2012, **4**, 699–704, DOI: 10.1038/nchem.1422.
88 J. Zhou, Y. Zuo, X. Wan, G. Long, Q. Zhang, W. Ni, Y. Liu, Z. Li, G. He, C. Li, B. Kan, M. Li and Y. Chen, *J. Am. Chem. Soc.*, 2013, **135**, 8484–8487, DOI: 10.1021/ja403318y.
89 Y. Sun, G. C. Welch, W. L. Leong, C. J. Takacs, G. C. Bazan and A. J. Heeger, *Nat. Mater.*, 2012, **11**, 44–48, DOI: 10.1038/nmat3160.
90 B. Walker, C. Kim and T. Nguyen, *Chem. Mater.*, 2011, **23**, 470–482, DOI: 10.1021/cm102189g.
91 Y. Lin, Y. Li and X. Zhan, *Chem. Soc. Rev.*, 2012, **41**, 4245–4272, DOI: 10.1039/c2cs15313k.
92 P. Sonar, J. P. F. Lim and K. L. Chan, *Energy Environ. Sci.*, 2011, **4**, 1558–1574, DOI: 10.1039/c0ee00668h.
93 J. Zhou, X. Wan, Y. Liu, Y. Zuo, Z. Li, G. He, G. Long, W. Ni, C. Li, X. Su and Y. Chen, *J. Am. Chem. Soc.*, 2012, **134**, 16345–16351, DOI: 10.1021/ja306865z.
94 V. Gupta, A. K. K. Kyaw, D. H. Wang, S. Chand, G. C. Bazan and A. J. Heeger, *Sci. Rep.*, 2013, **3**, 1965, DOI: 10.1038/srep01965.
95 M. Stolar and T. Baumgartner, *Phys. Chem. Chem. Phys.*, 2013, **15**, 9007–9024, DOI: 10.1039/c3cp51379c.
96 C. L. Chochos, N. Tagmatarchis and V. G. Gregoriou, *RSC Adv.*, 2013, **3**, 7160–7181, DOI: 10.1039/c3ra22926b.
97 J. E. Anthony, *Chem. Mater.*, 2011, **23**, 583–590, DOI: 10.1021/cm1023019.
98 J. E. Anthony, A. Facchetti, M. Heeney, S. R. Marder and X. Zhan, *Adv. Mater.*, 2010, **22**, 3876–3892, DOI: 10.1002/adma.200903628.
99 R. Y. C. Shin, T. Kietzke, S. Sudhakar, A. Dodabalapur, Z. Chen and A. Sellinger, *Chem. Mater.*, 2007, **19**, 1892–1894, DOI: 10.1021/cm070144d.
100 Z. E. Ooi, T. L. Tam, R. Y. C. Shin, Z. K. Chen, T. Kietzke, A. Sellinger, M. Baumgarten, K. Mullen and J. C. deMello, *J. Mater. Chem.*, 2008, **18**, 4619–4622, DOI: 10.1039/b813786m.
101 R. Y. C. Shin, P. Sonar, P. S. Siew, Z. Chen and A. Sellinger, *J. Org. Chem.*, 2009, **74**, 3293–3298, DOI: 10.1021/jo802720m.
102 C. H. Woo, T. W. Holcombe, D. A. Unruh, A. Sellinger and J. M. J. Fréchet, *Chem. Mater.*, 2010, **22**, 1673–1679, DOI: 10.1021/cm903067a.
103 E. Lim, S. Lee and K. K. Lee, *Mol. Cryst. Liq. Cryst.*, 2012, **565**, 98–105, DOI: 10.1080/15421406.2012.693285.
104 D. A. M. Egbe, H. Neugebauer and N. S. Sariciftci, *J. Mater. Chem.*, 2011, **21**, 1338–1349, DOI: 10.1039/c0jm02429e.
105 J. T. Bloking, X. Han, A. T. Higgs, J. P. Kastrop, L. Pandey, J. E. Norton, C. Risko, C. E. Chen, J. Bredas, M. D. McGehee and A. Sellinger, *Chem. Mater.*, 2011, **23**, 5484–5490, DOI: 10.1021/cm203111k.

106 L. Ding, H. Ying, Y. Zhou, T. Lei and J. Pei, *Org. Lett.*, 2010, **12**, 5522–5525, DOI: 10.1021/ol1024103.
107 Y. Zhou, L. Ding, K. Shi, Y. Dai, N. Ai, J. Wang and J. Pei, *Adv. Mater.*, 2012, **24**, 957–961, DOI: 10.1002/adma.201103927.
108 Y. Zhou, Y. Dai, Y. Zheng, X. Wang, J. Wang and J. Pei, *Chem. Commun.*, 2013, **49**, 5802–5804, DOI: 10.1039/c3cc41803k.
109 L. Ding, H. Li, T. Lei, H. Ying, R. Wang, Y. Zhou, Z. Su and J. Pei, *Chem. Mater.*, 2012, **24**, 1944–1949, DOI: 10.1021/cm300747v.
110 P. E. Schwenn, K. Gui, A. M. Nardes, K. B. Krueger, K. H. Lee, K. Mutkins, H. Rubinstein-Dunlop, P. E. Shaw, N. Kopidakis, P. L. Burn and P. Meredith, *Adv. Energy Mater.*, 2011, **1**, 73–81, DOI: 10.1002/aenm.201000024.
111 Y. Kim, S. Cook, S. Choulis, J. Nelson, J. Durrant and D. Bradley, *Chem. Mater.*, 2004, **16**, 4812–4818, DOI: 10.1021/cm049585c.
112 K. Gui, K. Mutkins, P. E. Schwenn, K. B. Krueger, A. Pivrikas, P. Wolfer, N. S. Stutzmann, P. L. Burn and P. Meredith, *J. Mater. Chem.*, 2012, **22**, 1800–1806, DOI: 10.1039/c1jm14089b.
113 K. B. Krueger, P. E. Schwenn, K. Gui, A. Pivrikas, P. Meredith and P. L. Burn, *Appl. Phys. Lett.*, 2011, **98**, 083301, DOI: 10.1063/1.3556280.
114 Y. Fang, A. K. Pandey, A. M. Nardes, N. Kopidakis, P. L. Burn and P. Meredith, *Adv. Energy Mater.*, 2013, **3**, 54–59, DOI: 10.1002/aenm.201200372.
115 P. Wolfer, P. E. Schwenn, A. K. Pandey, Y. Fang, N. Stingelin, P. L. Burn and P. Meredith, *J. Mater. Chem. A*, 2013, **1**, 5989–5995, DOI: 10.1039/c3ta10554g.
116 K. N. Winzenberg, P. Kemppinen, F. H. Scholes, G. E. Collis, Y. Shu, T. B. Singh, A. Bilic, C. M. Forsyth and S. E. Watkins, *Chem. Commun.*, 2013, **49**, 6307–6309, DOI: 10.1039/c3cc42293c.
117 H. Yan, Z. Chen, Y. Zheng, C. Newman, J. R. Quinn, F. Dotz, M. Kastler and A. Facchetti, *Nature*, 2009, **457**, 679-U1, DOI: 10.1038/nature07727.
118 L. E. Polander, S. P. Tiwari, L. Pandey, B. M. Seifried, Q. Zhang, S. Barlow, C. Risko, J. Bredas, B. Kippelen and S. R. Marder, *Chem. Mater.*, 2011, **23**, 3408–3410, DOI: 10.1021/cm201729s.
119 E. Ahmed, G. Ren, F. S. Kim, E. C. Hollenbeck and S. A. Jenekhe, *Chem. Mater.*, 2011, **23**, 4563–4577, DOI: 10.1021/cm2019668.
120 G. Ren, E. Ahmed and S. A. Jenekhe, *Adv. Energy Mater.*, 2011, **1**, 946–953, DOI: 10.1002/aenm.201100285.
121 G. Ren, E. Ahmed and S. A. Jenekhe, *J. Mater. Chem.*, 2012, **22**, 24373–24379, DOI: 10.1039/c2jm33787h".
122 H. Li, F. S. Kim, G. Ren, E. C. Hollenbeck, S. Subramaniyan and S. A. Jenekhe, *Angew. Chem., Int. Ed.*, 2013, **52**, 5513–5517, DOI: 10.1002/anie.201210085.
123 B. Walker, A. B. Tomayo, X. Dang, P. Zalar, J. H. Seo, A. Garcia, M. Tantiwiwat and T. Nguyen, *Adv. Funct. Mater.*, 2009, **19**, 3063–3069, DOI: 10.1002/adfm.200900832.
124 S. Qu and H. Tian, *Chem. Commun.*, 2012, **48**, 3039–3051, DOI: 10.1039/c2cc17886a.
125 J. C. Bijleveld, A. P. Zoombelt, S. G. J. Mathijssen, M. M. Wienk, M. Turbiez, D. M. de Leeuw and R. A. J. Janssen, *J. Am. Chem. Soc.*, 2009, **131**, 16616–16617, DOI: 10.1021/ja907506r.
126 P. Sonar, G. Ng, T. T. Lin, A. Dodabalapur and Z. Chen, *J. Mater. Chem.*, 2010, **20**, 3626–3636, DOI: 10.1039/b924404b.
127 Y. Lin, P. Cheng, Y. Li and X. Zhan, *Chem. Commun.*, 2012, **48**, 4773–4775, DOI: 10.1039/c2cc31511d.
128 H. Usta, G. Lu, A. Facchetti and T. J. Marks, *J. Am. Chem. Soc.*, 2006, **128**, 9034–9035, DOI: 10.1021/ja062908g.
129 P. T. Boudreault, A. Michaud and M. Leclerc, *Macromol. Rapid Commun.*, 2007, **28**, 2176–2179, DOI: 10.1002/marc.200700470.
130 E. Kozma and M. Catellani, *Dyes Pigm.*, 2013, **98**, 160, DOI: 10.1016/j.dyepig.2013.01.020.
131 S. Rajaram, R. Shivanna, S. K. Kandappa and K. S. Narayan, *J. Phys. Chem. Lett.*, 2012, **3**, 2405–2408, DOI: 10.1021/jz301047d.
132 J. J. Dittmer, E. A. Marseglia and R. H. Friend, *Adv. Mater.*, 2000, **12**, 1270–1274, DOI: 10.1002/1521-4095(200009)12:17<1270:aid-adma1270>3.0.co;2-8.
133 J. J. Dittmer, K. Petritsch, E. A. Marseglia, R. H. Friend, H. Rost and A. B. Holmes, *Synth. Met.*, 1999, **102**, 879, DOI: 10.1016/s0379-6779(98)00852-2".
134 B. A. Jones, A. Facchetti, M. R. Wasielewski and T. J. Marks, *J. Am. Chem. Soc.*, 2007, **129**, 15259–15278, DOI: 10.1021/ja075242e.
135 I. Kim, H. M. Haverinen, Z. Wang, S. Madakuni, J. Li and G. E. Jabbour, *Appl. Phys. Lett.*, 2009, **95**, 023305, DOI: 10.1063/1.3177349.
136 B. A. Gregg, *J. Phys. Chem.*, 1996, **100**, 852–859, DOI: 10.1021/jp952557k.
137 W. S. Shin, H. Jeong, M. Kim, S. Jin, M. Kim, J. Lee, J. W. Lee and Y. Gal, *J. Mater. Chem.*, 2006, **16**, 384–390, DOI: 10.1039/b512983d".
138 I. Kim and G. E. Jabbour, *Synth. Met.*, 2012, **162**, 102, DOI: 10.1016/j.synthmet.2011.11.018".
139 S. H. Oh, B. G. Kim, S. J. Yun, M. Maheswara, K. Kim and J. Y. Do, *Dyes Pigm.*, 2010, **85**, 37–42, DOI: 10.1016/j.dyepig.2009.10.001.
140 B. R. Sim, B. Kim, J. K. Lee and J. Y. Do, *Thin Solid Films*, 2011, **519**, 8091–8094, DOI: 10.1016/j.tsf.2011.04.127.
141 X. Zhang, Z. Lu, L. Ye, C. Zhan, J. Hou, S. Zhang, B. Jiang, Y. Zhao, J. Huang, S. Zhang, Y. Liu, Q. Shi, Y. Liu and J. Yao, *Adv. Mater.*, 2013, **25**, 5791–5797, DOI: 10.1002/adma.201300897.
142 Q. Yan, Y. Zhou, Y. Zheng, J. Pei and D. Zhao, *Chem. Sci.*, 2013, **4**, 4389–4394, DOI: 10.1039/c3sc51841h.
143 M. P. Krafft and J. G. Riess, *Chem. Rev.*, 2009, **109**, 1714–1792.
144 Y. Huang, G. C. Welch, G. C. Bazan, M. L. Chabinyc and W. Su, *Chem. Commun.*, 2012, **48**, 7250–7252, DOI: 10.1039/c2cc32401f.
145 T. P. Osedach, T. L. Andrew and V. Bulovic, *Energy Environ. Sci.*, 2013, **6**, 711–718, DOI: 10.1039/c3ee24138f.